Repurposing of auranofin: Thioredoxin reductase remains a primary target of the drug

Xiaonan Zhang, Karthik Selvaraj, Amir Ata Saei, Padraig D´arcy, Roman A. Zubarev, Elias S. J. Arner and Stig Linder

Zhang, X., Selvaraj, K., Saei, A. A., D´arcy, P., Zubarev, R. A., Arner, E. S. J., Linder, S., (2019), Repurposing of auranofin: Thioredoxin reductase remains a primary target of the drug, *Biochimie*, 162, 46-54. https://doi.org/10.1016/j.biochi.2019.03.015

Original publication available at:
https://doi.org/10.1016/j.biochi.2019.03.015

Repurposing of auranofin: thioredoxin reductase remains a primary target of the drug

Xiaonan Zhang[1], Karthik Selvaraju[2], Amir Ata Saei[3], Padraig D'Arcy[2], Roman A Zubarev[3], Elias SJ Arnér[4] and Stig Linder[1,2]

[1] Department of Oncology-Pathology, Karolinska Institutet, SE-171 76 Stockholm;

[2] Department of Medical and Health Sciences, Linköping University, SE-581 83 Linköping;

[3] Department of Medical Biochemistry and Biophysics, Division of Physiological Chemistry I, Karolinska Institutet, SE-171 77, Stockholm, Sweden.

[4] Division of Biochemistry, Department of Medical Biochemistry and Biophysics, Karolinska Institute, SE-171 77 Stockholm.

Key words: auranofin; proteasome deubiquitinases; thioredoxin reductase; selenocysteine

* Corresponding author: Stig Linder, Department of Medical and Health Sciences, Linköping University and Department of Oncology-Pathology, Karolinska Institute, Stockholm, Sweden. Email: Stig.Linder@ki.se and Stig.Linder@liu.se

Abstract

Auranofin is a gold (I)-containing compound used for the treatment of rheumatic arthritis. Auranofin has anticancer activity in animal models and is approved for clinical trials for lung and ovarian carcinomas. Both the cytosolic and mitochondrial forms of the selenoprotein thioredoxin reductase (TrxR) are well documented targets of auranofin. Auranofin was recently reported to inhibit proteasome activity at the level of the proteasome-associated deubiquitinases (DUBs) UCHL5 and USP14. We here set out to re-examine the molecular mechanism underlying auranofin cytotoxicity towards cultured cancer cells. The effects of auranofin on the proteasome was examined in cells and *in vitro*, effects on DUB activity was assessed using different substrates. The cellular response to auranofin was compared to that of the 20S proteasome inhibitor bortezomib and the 19S DUB inhibitor b-AP15 using proteomics. Auranofin was found to inhibit mitochondrial activity and to induce oxidative stress response at IC_{50} doses. At 2 - 3-fold higher doses, auranofin inhibits proteasome processing in cells. At such supra-pharmacological concentrations USP14 activity was inhibited. Analysis of protein expression profiles in drug-exposed tumor cells showed that auranofin induces a response distinct from that of the 20S proteasome inhibitor bortezomib and the DUB inhibitor b-AP15, both of which induced similar responses. Our results support the notion that the primary mechanism of action of auranofin is TrxR inhibition and suggest that proteasome DUB inhibition is an off-target effect. Whether proteasome inhibition will contribute to the antineoplastic effect of auranofin in treated patients is unclear but remains a possibility.

Abbreviations

ALSL1: Acetolactate Synthase; **AUF:** Auranofin; **CP:** Core Particle; **DTT:** Dithiothreitol; **DUB:** Deubiquitinase Enzyme; **FDA:** U.S. Food and Drug Administration; **HMOX:** Hemeoxygenase-1; **K48:** Lysine 48; **Nrf2:** Nuclear factor E2-Related Factor 2; **POH1/Rpn11:** Pad1 Homologue, proteasome 26S subunit, non-ATPase 14; **PVDF:** Polyvinylidene difluoride; **ROS:** Reactive oxygen species; **Sec:** Selenocysteine; **SFXN4:** Sideroflexin 4; **TFA:** Trifluoroacetic acid; **TrxR:** Thioredoxin Reductase; **UCHL5:** Ubiquitin C-terminal Hydrolase L5; **UPS:** Ubiquitin-Proteasome System; **USP14:** Ubiquitin Specific Protease 14; **Ub-VS:** Ubiquitin-vinylsulfone; **YFP:** Yellow Fluorescent Protein.

1. Introduction

Cellular reduction-oxidation (redox) systems are indispensable for life and affect many aspects of biological functions in mammalian cells [1]. In cancer cells, elevated levels of ROS are frequently observed and have pivotal roles in the acquisition of the hallmarks of cancer [2], enhancing tumor cell proliferation, metastasis and disruption of cell death signaling [3]. Simultaneously, protective redox systems are accordingly upregulated in cancer cells, often through activation of the transcription factor Nrf2, to prevent the damages of excessive ROS and to maintain the redox balance [4, 5].

Auranofin (AUF) is a gold (I)-containing phosphine compound that is approved by FDA for treatment of rheumatoid arthritis [6]. Auranofin targets thioredoxin reductase (TrxR), both the cytosolic form TrxR1 and the mitochondrial form TrxR2 [7, 8]. TrxR isoforms are selenoproteins with an easily accessible and highly nucleophilic active site selenocysteine residue, which make them especially prone to irreversible inhibition by auranofin [9, 10]. Auranofin-induced cell death of cancer cells is associated with excessive levels of oxidative stress and impaired reductive pathways in both cytosol and mitochondria [7, 11, 12]. Auranofin shows cytotoxicity to human chronic leukemia and gastric cancer cells which is associated with mitochondrial dysfunction and ROS overproduction [13, 14]. Clinical trials of auranofin for ovarian cancer (NCT03456700), chronic lymphocytic leukemia (CLL, NCT03456700) and lung cancer (NCT03456700) are ongoing or have been completed. Furthermore, auranofin displays activities which may or may not relate to TrxR inhibition, including the inhibition of protein tyrosine phosphatases [15], deubiquitinases [16] and selenium metabolism [17].

The ubiquitin-proteasome system (UPS) is essential for protein quality control and stress survival [18]. Proteins targeted for removal are first conjugated with ubiquitin and in the form of polyubiquitinated proteins then transferred to the 26S proteasome where degradation occurs [19]. Following binding to receptors at the 19S proteasome, polyubiquitin chains are removed by deubiquitinase enzymes (DUBs) that are localized in the 19S regulatory particles (19S RP). Two of these enzymes are cysteine proteases (USP14 and UCHL5) and a third is a metalloprotease (POH1/Rpn11). Deubiquitinated protein substrates are then translocated into the 20S core particle (20S CP) where the caspase, trypsin and chymotrypsin-like activities cleave the proteins into small peptides [19, 20].

Targeting the various components of the UPS has become a promising strategy for cancer therapies [21]. However, so far, the only drugs that have been approved for clinical use are inhibitors of the 20S proteasome (bortezomib, carfilzomib and ixazomib) [21], approved for hematological diseases, primarily multiple myeloma. The lack of efficacy on solid tumors has narrowed the application of bortezomib [22], and acquired resistance constitutes a significant clinical problem [23]. Alternative targets that may be exploited such as 19S DUB enzymes [24, 25] and 19S ubiquitin receptors [26] have thus attracted widespread interest. The reports that auranofin acts as a proteasome inhibitor by direct targeting of the proteasome-associated cysteine DUBs [16, 27] are important in this context. Auranofin induces apoptosis of multiple myeloma cells *in vitro* [28] and could possibly be repurposed for treatment of bortezomib-resistant myeloma. We here examined the response of cultured cancer cells to auranofin, aiming to determine whether the primary mechanism of cytotoxicity of this drug is related to proteasome inhibition.

2. Materials and methods

2.1. Chemicals and antibodies

b-AP15 was obtained from OnTarget Chemistry (Uppsala, Sweden), Auranofin (Sigma-Aldrich) and Velcade (bortezomib, Selleck Chem). Antibodies used were anti-actin (Sigma-Aldrich catalogue number A5441), anti-tubulin (Sigma-Aldrich catalogue number T4026), anti-Ub-K48 (Merck Millipore catalogue number 05-1307), anti-HMOX (BD Bioscience catalogue number 610713), anti-USP14 (A300-920A), anti-UCHL5 (A304-099A) (Bethyl Laboratories, Inc., Montgomery, TX, USA). Anti-HA-TAG (3724T), PSMD14 (4197S), PSMC2 (14395S), PSMD4 (3336S), PSMA2 (2455S) and Nrf2 (12721) were obtained from Cell signaling technology.

2.2. Cell culture

HCT116 colon carcinoma cells were maintained in McCoy´s 5A modified medium with 10% FBS and 1% penicillin. HeLa cells, MelJuSo- Ub^{G76V}-YFP cells and HEK293 cells were cultured in DMEM medium supplemented with 10% FBS and 1% penicillin. Cell lines were used at low passage numbers and checked for absence of mycoplasma.

2.3. Western blot analysis

Cell extract proteins were resolved by 3-8% Tris-Acetate protein gels (Invitrogen, Carlsbad, CA) to detect polyubiquitinated proteins and 4-12% Bis-Tris protein gels to detect other proteins mentioned in the text, then transferred onto a PVDF membrane for western blotting. Blots were developed by enhanced chemiluminescence (Amersham, Arlington Heights, IL).

2.4. Measurements of oxygen consumption and extracellular acidification

The Seahorse XF analyser was used as recommended by the manufacturer (Seahorse Bioscience, North Billerica, MA, USA). 60,000 cells/well were plated in 100 μL culture medium in XF24-well cell plates with blank control wells. Before the measurements, the

medium was replaced with 500 µl Seahorse assay media (1 mM pyruvate, 25 mM glucose and 2 mM glutamine) at 37 °C without CO_2 for 1 h. OCR (oxygen consumption rate) and ECAR (extracellular acidification rate) values were measured by XF24 extracellular flux analyzer in real time as recommended by the manufacturer.

2.5. Live-cell analysis on MelJuSo- Ub^{G76V}-YFP /nucleus red cells

MelJuSo- Ub^{G76V}-YFP /nucleus red cells were plated in the 96-well plate overnight and then treated with various concentrations of auranofin (0.25, 0.5, 1 and 1.5 µM) and b-AP15. Treatment with compounds that block the UPS leads to accumulation of YFP in these cells and the generated fluorescence was continuously detected in an IncuCyte® FLR instrument (Essen BioScience Inc.).

2.6. Proteomics

After treatment with a drug at concentrations and durations given in the text, cells were collected, washed twice with PBS and then lysed using 8 M urea, 1% SDS, 50 mM Tris at pH 8.5 with protease inhibitors. The cell lysates were subjected to 1 min sonication on ice using Branson probe sonicator and 3 s on/off pulses with a 30% amplitude. Protein concentration was then measured for each sample using a BCA Protein Assay Kit (Thermo). 50 μg of each sample was reduced with DTT (final concentration 10 mM) for 1 h at room temperature. Afterwards, iodoacetamide was added to a final concentration of 50 mM. The samples were incubated in room temperature for 1 h in the dark, with the reaction being stopped by addition of 10 mM DTT. After precipitation of proteins using methanol/chloroform, the semi-dry protein pellet was dissolved in 25 μL of 8 M urea in 20 mM EPPS (pH 8.5) and was then diluted with EPPS buffer to reduce the urea concentration to 4 M. Lysyl Endopeptidase (Wako) was added at a 1: 100 w/w ratio to protein and incubated at room temperature overnight. After diluting urea to 1 M, trypsin (Promega) was added at the ratio of 1: 100 w/w

and the samples were incubated for 6 h at room temperature. TMT10 reagents were added 4x by weight to each sample, followed by incubation for 2 h at room temperature. The reaction was quenched by addition of 0.5% hydroxylamine. Samples were combined, acidified by TFA, cleaned using Sep-Pak (Waters) and dried using a DNA 120 SpeedVac™ concentrator (Thermo). Samples were then resuspended in 0.1% TFA and separated into 8 fractions using High pH Reversed-Phase Peptide Fractionation Kit (Thermo). After resuspension in 0.1% FA (Fluka), each fraction was analyzed with a 140 min gradient in random order. Samples in were loaded with buffer A (0.1% formic acid in water) onto a 50 cm EASY-Spray column (75 μm internal diameter, packed with PepMap C18, 2 μm beads, 100 Å pore size) connected to a nanoflow liquid chromatograph Dionex UltiMate 3000 (Thermo) and eluted with a buffer B (98% ACN, 0.1% FA, 2% H2O) gradient from 2% to 35% of at a flow rate of 250 nL/min. Mass spectra were acquired with an Orbitrap Elite mass spectrometer (Thermo) in the data-dependent mode at a nominal resolution of 30,000, in the m/z range from 375 to 1200. Peptide fragmentation was performed via higher-energy collision dissociation (HCD) with energy set at 35 NCE.

The raw data from LC-MS were analyzed by MaxQuant, version 1.5.6.5 [29]. The Andromeda search engine [30] searched MS/MS data against the International Protein Index (human, version UP000005640_9606, 92957 entries). Cysteine carbamidomethylation was used as a fixed modification, while methionine oxidation was selected as a variable modification. Trypsin/P and LysC/P were selected as enzyme specificity. No more than two missed cleavages were allowed. A 1% false discovery rate was used as a filter at both protein and peptide levels. For all other parameters, the default settings were used. After removing all the contaminants, only proteins with at least two peptides were included in the final dataset. Protein abundances were normalized by the total protein abundance in each sample.

2.7. Ub-VS labeling assay

Cell pellets collected from control or treated cells were lysed with buffer (50 mM HEPES pH 7.4, 250 mM sucrose, 10 mM $MgCl_2$, 2 mM ATP, 1 mM DTT and 1% NP-40) on ice for 30 min followed by centrifugation. Supernatants were collected and 25 μg of protein was labeled with 1 μM Ub-VS for 30 min at 37 °C. Samples were resolved by SDS-PAGE and subjected to immunoblotting.

2.8. 20S proteasome activity

In vitro proteasome activity assays were performed using 20S core particle (2 nM, from human cells, Boston Biochem) in reaction buffer (25 mM HEPES, 0.5 mM EDTA and 0.03% sodium dodecyl sulfate). 10 μM of the substrate Suc-LLVY-AMC was added for the detection of chymotrypsin-like activity using a multilabel counter equipped with 380-nm excitation and 460-nm emission filters.

2.9. Purification of proteasomes from HEK293 cells

Proteaselect-HEK293_Bio-Rpn11 cells (Ubiquigent Ltd, Dundee, Scotland) were treated with auranofin or b-AP15 for 6 hours, harvested and lysed in UbVS lysis buffer containing 2 mM ATP. After 20 min incubation, extracts were cleared by centrifugation at 10,000g for 10 min at 4 °C. Protein concentration was adjusted to 1 mg/mL and 1 mL was used for purification. Streptavidin magnetic beads (88816, Thermo Scientific, USA) as described by the vendor. Proteins were eluted by boiling for 5 mins at 95°C in SDS sample buffer, resolved by SDS–PAGE and subjected to immunoblotting.

2.10. Statistical analysis

Statistical significance was evaluated by Students two-tailed paired t-test (parametric), or Mann-Whitney U-test (non-parametric). Protein expression data were compared using Spearman correlation coefficients.

3. Results

3.1. Auranofin induces an oxidative stress response and mitochondrial dysfunction

Auranofin is a gold(I) phosphine compound (**Fig. 1a**) displaying a high affinity to the selenocysteine- (Sec-) containing redox active center Cys-495/SeCys-496 of thioredoxin reductase (TrxR) that is required for thioredoxin reduction by the enzyme. Exposure of cells to auranofin thereby indirectly targets the entire thioredoxin system (**Fig. 1b**). The IC_{50} concentration for auranofin in human HCT116 colon cancer cells is ~1.5 μM [12]. At this concentration, auranofin induced some accumulation of poly-ubiquitinated proteins within 6 hours of incubation (**Fig. 1c**), consistent with previous reports [16, 27]. The extent of poly-ubiquitinated protein accumulation was, however, much weaker compared to the effects of the 20S proteasome inhibitor bortezomib and the 19S DUB inhibitor b-AP15 (**Fig. 1c**) and was not observed in all experiments (see below). In contrast, strong induction of the expression of hemeoxygenase-1 (HMOX), a target of Nrf-2 and a marker of oxidative stress [31], was observed at this concentration of auranofin (**Fig. 1c**). Mitochondrial oxidative phosphorylation is impeded by auranofin [12, 32], an effect commonly attributed to the inhibition of the mitochondrial isoform TrxR2 [7]. We here found that cellular oxygen consumption was also severely impeded in HCT116 cells at a concentration of 1 μM

auranofin(**Fig. 1d**). The decrease in oxygen consumption was associated with increased extracellular acidification, compatible with mitochondrial dysfunction and anaerobic glycolysis (**Fig. 1e**).

3.2. Auranofin induces a phenotypic response distinct from proteasome inhibitors

Expression profiling, either at the RNA or protein level, is a useful approach for the evaluation of the molecular mechanism of action of pharmacological agents [33, 34]. We used shotgun proteomics to examine the response of HCT116 cells to 1.0 μM auranofin (**Fig. 2a**), a concentration sufficient to inhibit mitochondrial oxidative phosphorylation. Cells were exposed for 6 hours in order to capture early effects of drug treatment. The strongest auranofin-induced proteins were SFXN4 (sideroflexin 4, a protein involved in iron utilization in mitochondria), ALSL1 (acetolactate synthase) and HMOX. The expression profile of auranofin-exposed cells did not show any significant correlation to that of cells exposed to 20S inhibitor bortezomib or to the 19S DUB inhibitor b-AP15 (**Fig. 2a**). In contrast, the expression profiles induced by b-AP15 and bortezomib were significantly correlated ($y = 0.7077x+0.094$, $R^2 =0.86849$; $p < 0.00001$).

Exposure of HCT116 cells to bortezomib or b-AP15 resulted in cells becoming highly vacuolized after 12 hours, a phenomenon not observed during exposure to 1.0 μM auranofin (**Fig. 2b**). We also examined the accumulation of a proteasome-targeted fusion protein, Ub^{G76V}-YFP [35] in living melanoma cells using an IncuCyte® instrument. This protein is intrinsically unstable due to constitutive degradation by the proteasome and impairment of the UPS leads to an increased fluorescent signal. The effect of auranofin on the proliferation of human MelJuSo- Ub^{G76V}-YFP cells shown in **Fig. 2c**. We examined the connection between the cell death and the induction of YFP signals in auranofin- or b-AP15 treated

MelJuSo- Ub^{G76V}-YFP cells. Treatment with auranofin at a concentration of 1.0 μM resulted in the death of 33 cells during the observation period. Of these, 17 cells became YFP-positive whereas 16 cells did not show YFP fluorescence prior to cell death (**Fig. 2d**). In contrast, all 35 cells that died following exposure to 1.0 μM b-AP15 became YFP positive prior to cell death (**Fig. 2d**). These findings show that auranofin-induced cell death is not strictly correlated with proteasome inhibition, in contrast to the strong association between cell death and proteasome inhibition observed with b-AP15.

3.3. Increases of polyubiquitinated proteins at elevated auranofin concentrations

We considered the possibility that supra-pharmacological concentrations of auranofin may have more profound effects on proteasome function. We indeed found that exposure of HCT116 cells to auranofin concentrations of ≥ 2.5 μM resulted in strong accumulation of K48-linked polyubiquitinated proteins (**Fig. 3a**). Auranofin was found to induce increased levels of chaperones at a concentration of 5 μM, whereas no such increases were observed at 1 μM (**Fig. 3b**). In contrast, the oxidative stress marker HMOX was induced by 0.25 μM auranofin in HCT116 cells (**Fig. 3a**). These results show that the oxidative stress-response and the effects on the UPS by auranofin can be separated.

3.4. Inhibition of USP14 by supra-pharmacological doses of auranofin

We examined different possibilities that may explain the accumulation of polyubiquitin at high (> IC_{50}) auranofin doses. We first considered the possibility that auranofin treatment leads to the dissociation of proteasome subunits, a phenomenon reported to occur during oxidative stress [36]. A cell line where the Rpn11/PSMD14 component of the 19S subunit contains a histidine and biotin purification tag (HEK293-Bio-Rpn11) was used to examine this

possibility [37]. The cysteine DUBs USP14 and UCHL5 were both pulled-down with Rpn11, as was the 19S base AAA-ATPase PSMC2 and the ubiquitin receptor PSMD4 (**Fig. 4a**). Importantly, the 20S core particle protein PSMA2 was also pulled-down, showing that auranofin did not induce dissociation of 19S and 20S subunits (**Fig. 4a**). We also examined whether proteasome 20S enzymatic activity was inhibited by auranofin. Treatment of purified proteasomes with doses of up to 20 μM auranofin did not result in detectable inhibition (**Fig. 4b**). Considering previous reports [16] we further investigated whether auranofin inhibits proteasome DUBs (USP14/UCHL5) of the 19S regulatory particle. These experiments were performed using cell extracts from cells exposed to auranofin for 6 hours and using the activity-based probe HA-UbVS [38]. Whereas no inhibition of USP14 labeling was observed at a concentration of 1.5 μM auranofin, reduced labeling was observed at 5 μM (**Fig. 4c**). UCHL5 labeling was less affected by the drug (**Fig. 4c**).

The accumulation of polyubiquitinated proteins and the increased expression of chaperones observed at 5 μM auranofin suggested that the drug may induce a cellular response characteristic of proteasome inhibitors at this concentration. However, analysis of global protein expression using proteomics showed that although 5 μM auranofin resulted in more pronounced alterations in protein expression compared to 1 μM, the responses were nevertheless distinct from those observed with b-AP15 and bortezomib (**Fig. 4d, Fig. 2a**).

4. Discussion

The present study was performed in order to examine whether the molecular mechanism of cytostatic action of auranofin is similar to, or closely overlaps with, that of previously described proteasome and deubiquitinase inhibitors. We were able to reproduce previous

findings of inhibition of proteasome processing by auranofin [16] as evidenced by the accumulation of K48-linked polyubiquitinated proteasome substrates in cells. However, strong accumulation of polyubiquitinated proteasome substrates required concentrations of 2.5 to 5 μM auranofin, i.e. higher than the IC_{50} dose inducing cytotoxicity. In contrast, induction of the Nrf2 target HMOX and inhibition of mitochondrial oxidative phosphorylation were observed at lower concentrations ($\leq$ 1 μM) previously also reported to lead to TrxR inhibition in HCT116 cells [12].

The phenotypic response to auranofin in terms of the profile of polypeptide expression was clearly distinct from that of the 20S proteasome inhibitor bortezomib and the 19S proteasome inhibitor b-AP15, both at the concentration of 1 μM and the higher concentration of 5 μM. Therefore, even at the concentration where poly-ubiquitin accumulation does occur, auranofin does not induce a cellular response typical of proteasome inhibition. In contrast, the profiles of polypeptide expression observed in cells exposed to bortezomib and b-AP15 were similar to each other and consistent with previous data using microarrays [39], supporting previous data that proteasome inhibition constitutes the dominant molecular mechanism of action of b-AP15 [40]. Our imaging studies using cells expressing a proteasome-degradable reporter showed that auranofin-induced cell death was not consistently preceded by detectable proteasome inhibition, supporting the notion that the molecular mechanism of action of auranofin-induced cell death is not primarily due to effects on the proteasome.

Three different mechanisms may explain the accumulation of K48-linked polyubiquitinated proteins in auranofin-treated cells: either direct targeting of components of the UPS, inhibition of some yet unidentified TrxR-dependent process in the UPS, or indirect effects due to induction of oxidative stress. The finding that expression of the Nrf2 target protein HMOX

was induced at a concentration almost one order of magnitude lower than that required for increases of K48-linked polyubiquitinated proteins (**Fig. 3a**) is not consistent with the hypothesis that a general increase in oxidative stress results in inhibition of proteasome activity. A direct link between TrxR1 targeting and HMOX induction has also been known for a long time [41]. We were able to demonstrate that auranofin directly inhibits the activity of the cysteine DUB USP14, consistent with previous reports [16]. This inhibition was observed at the same supra-cytotoxic doses that resulted in a broad accumulation of proteasome substrates. We could, however, not detect any direct inhibition of 20S proteasome activity or dissociation of proteasome subunits, but since auranofin is a potentially reactive drug other direct effects on the UPS should not be excluded.

4. Conclusions

We conclude that TrxR inhibition, associated with oxidative stress in cancer cells and associated with mitochondrial dysfunction, is likely to be the dominant mechanism underlying auranofin cytotoxicity. Proteasome inhibition occurs at relatively high concentrations of auranofin and may be due, at least in part, to inhibition of the cysteine DUB USP14. Auranofin is orally bioavailable [42] and its pharmacokinetic indicates a steady-state plasma concentrations and half-life in the order of 20 days [43]. It remains to be established whether sufficiently high auranofin concentrations can be achieved *in vivo* to target the UPS, but it is well known that gold (I)-containing compounds can yield prolonged TrxR inhibition *in vivo*. Since lower doses of auranofin are sufficient to inhibit TrxR and since TrxR inhibition *per se* is sufficient to elicit toxicity to cancer cells and neoplastic effects *in vivo* [12], we find it most likely that the molecular mode of action also *in vivo* is inhibition of TrxR.

Conflict of interest

SL is a consultant of Vivolux AB. No other potential conflicts of interest were disclosed.

Authors' Contributions

Conception and design: X.Z., E.A. and S.L.; Acquisition of data: X.Z., K.S. and A.S.; Analysis and interpretation of data: X.Z., K.S. and A.S.. The manuscript was written by X.Z. and S.L. and reviewed/revised by X.Z., K.S., A.S., P.D., R.Z., E.A. and S.L..

Acknowledgements

The study was supported by the Swedish Cancer Society, Radiumhemmets forskningsfonder, Vetenskapsrådet, Barncancerfonden, Knut and Alice Wallenbergs Foundation.

References

[1] S. Soh, M. Byrska, K. Kandere-Grzybowska, B.A. Grzybowski, Reaction-diffusion systems in intracellular molecular transport and control, Angew Chem Int Ed Engl, 49 (2010) 4170-4198.
[2] D. Hanahan, R.A. Weinberg, The hallmarks of cancer, Cell, 100 (2000) 57-70.
[3] S.S. Sabharwal, P.T. Schumacker, Mitochondrial ROS in cancer: initiators, amplifiers or an Achilles' heel?, Nat Rev Cancer, 14 (2014) 709-721.
[4] D. Trachootham, J. Alexandre, P. Huang, Targeting cancer cells by ROS-mediated mechanisms: a radical therapeutic approach?, Nat Rev Drug Discov, 8 (2009) 579-591.
[5] M. Yamamoto, T.W. Kensler, H. Motohashi, The KEAP1-NRF2 System: a Thiol-Based Sensor-Effector Apparatus for Maintaining Redox Homeostasis, Physiol Rev, 98 (2018) 1169-1203.
[6] J.M. Madeira, D.L. Gibson, W.F. Kean, A. Klegeris, The biological activity of auranofin: implications for novel treatment of diseases, Inflammopharmacology, 20 (2012) 297-306.
[7] V. Gandin, A.P. Fernandes, M.P. Rigobello, B. Dani, F. Sorrentino, F. Tisato, M. Bjornstedt, A. Bindoli, A. Sturaro, R. Rella, C. Marzano, Cancer cell death induced by phosphine gold(I) compounds targeting thioredoxin reductase, Biochemical pharmacology, 79 (2010) 90-101.
[8] O. Rackham, A.M. Shearwood, R. Thyer, E. McNamara, S.M. Davies, B.A. Callus, A. Miranda-Vizuete, S.J. Berners-Price, Q. Cheng, E.S. Arner, A. Filipovska, Substrate and inhibitor specificities differ between human cytosolic and mitochondrial thioredoxin reductases: Implications for development of specific inhibitors, Free Radic Biol Med, 50 (2011) 689-699.
[9] M.P. Rigobello, A. Folda, M.C. Baldoin, G. Scutari, A. Bindoli, Effect of auranofin on the mitochondrial generation of hydrogen peroxide. Role of thioredoxin reductase, Free Radic Res, 39 (2005) 687-695.
[10] M.P. Rigobello, G. Scutari, A. Folda, A. Bindoli, Mitochondrial thioredoxin reductase inhibition by gold(I) compounds and concurrent stimulation of permeability transition and release of cytochrome c, Biochemical pharmacology, 67 (2004) 689-696.
[11] E.S.J. Arner, Targeting the Selenoprotein Thioredoxin Reductase 1 for Anticancer Therapy, Adv Cancer Res, 136 (2017) 139-151.
[12] W.C. Stafford, X. Peng, M.H. Olofsson, X. Zhang, D.K. Luci, L. Lu, Q. Cheng, L. Tresaugues, T.S. Dexheimer, N.P. Coussens, M. Augsten, H.M. Ahlzen, O. Orwar, A. Ostman, S. Stone-Elander, D.J. Maloney, A. Jadhav, A. Simeonov, S. Linder, E.S.J. Arner, Irreversible inhibition of cytosolic thioredoxin reductase 1 as a mechanistic basis for anticancer therapy, Science translational medicine, 10 (2018).
[13] W. Fiskus, N. Saba, M. Shen, M. Ghias, J. Liu, S.D. Gupta, L. Chauhan, R. Rao, S. Gunewardena, K. Schorno, C.P. Austin, K. Maddocks, J. Byrd, A. Melnick, P. Huang, A. Wiestner, K.N. Bhalla, Auranofin induces lethal oxidative and endoplasmic reticulum stress and exerts potent preclinical activity against chronic lymphocytic leukemia, Cancer Res, 74 (2014) 2520-2532.
[14] P. Zou, M. Chen, J. Ji, W. Chen, X. Chen, S. Ying, J. Zhang, Z. Zhang, Z. Liu, S. Yang, G. Liang, Auranofin induces apoptosis by ROS-mediated ER stress and mitochondrial dysfunction and displayed synergistic lethality with piperlongumine in gastric cancer, Oncotarget, 6 (2015) 36505-36521.
[15] D. Krishnamurthy, M.R. Karver, E. Fiorillo, V. Orru, S.M. Stanford, N. Bottini, A.M. Barrios, Gold(I)-mediated inhibition of protein tyrosine phosphatases: a detailed in vitro and cellular study, Journal of medicinal chemistry, 51 (2008) 4790-4795.

[16] N. Liu, X. Li, H. Huang, C. Zhao, S. Liao, C. Yang, S. Liu, W. Song, X. Lu, X. Lan, X. Chen, S. Yi, L. Xu, L. Jiang, C. Zhao, X. Dong, P. Zhou, S. Li, S. Wang, X. Shi, P.Q. Dou, X. Wang, J. Liu, Clinically used antirheumatic agent auranofin is a proteasomal deubiquitinase inhibitor and inhibits tumor growth, Oncotarget, 5 (2014) 5453-5471.
[17] S. Talbot, R. Nelson, W.T. Self, Arsenic trioxide and auranofin inhibit selenoprotein synthesis: implications for chemotherapy for acute promyelocytic leukaemia, British journal of pharmacology, 154 (2008) 940-948.
[18] D. Finley, Recognition and processing of ubiquitin-protein conjugates by the proteasome, Annu Rev Biochem, 78 (2009) 477-513.
[19] A. Hershko, A. Ciechanover, The ubiquitin system, Annu Rev Biochem, 67 (1998) 425-479.
[20] M. Rechsteiner, L. Hoffman, W. Dubiel, The multicatalytic and 26 S proteases, J Biol Chem, 268 (1993) 6065-6068.
[21] C.S. Chim, S.K. Kumar, R.Z. Orlowski, G. Cook, P.G. Richardson, M.A. Gertz, S. Giralt, M.V. Mateos, X. Leleu, K.C. Anderson, Management of relapsed and refractory multiple myeloma: novel agents, antibodies, immunotherapies and beyond, Leukemia, 32 (2018) 252-262.
[22] T. Caravita, P. de Fabritiis, A. Palumbo, S. Amadori, M. Boccadoro, Bortezomib: efficacy comparisons in solid tumors and hematologic malignancies, Nat Clin Pract Oncol, 3 (2006) 374-387.
[23] D. Niewerth, G. Jansen, Y.G. Assaraf, S. Zweegman, G.J. Kaspers, J. Cloos, Molecular basis of resistance to proteasome inhibitors in hematological malignancies, Drug resistance updates : reviews and commentaries in antimicrobial and anticancer chemotherapy, 18 (2015) 18-35.
[24] P. D'Arcy, S. Linder, Molecular pathways: translational potential of deubiquitinases as drug targets, Clinical cancer research : an official journal of the American Association for Cancer Research, 20 (2014) 3908-3914.
[25] L. Lauinger, J. Li, A. Shostak, I.A. Cemel, N. Ha, Y. Zhang, P.E. Merkl, S. Obermeyer, N. Stankovic-Valentin, T. Schafmeier, W.J. Wever, A.A. Bowers, K.P. Carter, A.E. Palmer, H. Tschochner, F. Melchior, R.J. Deshaies, M. Brunner, A. Diernfellner, Thiolutin is a zinc chelator that inhibits the Rpn11 and other JAMM metalloproteases, Nature chemical biology, (2017).
[26] R.K. Anchoori, B. Karanam, S. Peng, J.W. Wang, R. Jiang, T. Tanno, R.Z. Orlowski, W. Matsui, M. Zhao, M.A. Rudek, C.F. Hung, X. Chen, K.J. Walters, R.B. Roden, A bis-benzylidine piperidone targeting proteasome ubiquitin receptor RPN13/ADRM1 as a therapy for cancer, Cancer cell, 24 (2013) 791-805.
[27] X. Chen, Q. Yang, L. Xiao, D. Tang, Q.P. Dou, J. Liu, Metal-based proteasomal deubiquitinase inhibitors as potential anticancer agents, Cancer Metastasis Rev, 36 (2017) 655-668.
[28] A. Nakaya, M. Sagawa, A. Muto, H. Uchida, Y. Ikeda, M. Kizaki, The gold compound auranofin induces apoptosis of human multiple myeloma cells through both down-regulation of STAT3 and inhibition of NF-kappaB activity, Leukemia research, 35 (2011) 243-249.
[29] J. Cox, M. Mann, MaxQuant enables high peptide identification rates, individualized p.p.b.-range mass accuracies and proteome-wide protein quantification, Nature biotechnology, 26 (2008) 1367-1372.
[30] J. Cox, N. Neuhauser, A. Michalski, R.A. Scheltema, J.V. Olsen, M. Mann, Andromeda: a peptide search engine integrated into the MaxQuant environment, Journal of proteome research, 10 (2011) 1794-1805.

[31] R.S. Hamamura, J.H. Ohyashiki, R. Kurashina, C. Kobayashi, Y. Zhang, T. Takaku, K. Ohyashiki, Induction of heme oxygenase-1 by cobalt protoporphyrin enhances the antitumour effect of bortezomib in adult T-cell leukaemia cells, Br J Cancer, 97 (2007) 1099-1105.
[32] F. Radenkovic, O. Holland, J.J. Vanderlelie, A.V. Perkins, Selective inhibition of endogenous antioxidants with Auranofin causes mitochondrial oxidative stress which can be countered by selenium supplementation, Biochemical pharmacology, 146 (2017) 42-52.
[33] J. Lamb, E.D. Crawford, D. Peck, J.W. Modell, I.C. Blat, M.J. Wrobel, J. Lerner, J.P. Brunet, A. Subramanian, K.N. Ross, M. Reich, H. Hieronymus, G. Wei, S.A. Armstrong, S.J. Haggarty, P.A. Clemons, R. Wei, S.A. Carr, E.S. Lander, T.R. Golub, The Connectivity Map: using gene-expression signatures to connect small molecules, genes, and disease, Science, 313 (2006) 1929-1935.
[34] M. Muroi, S. Kazami, K. Noda, H. Kondo, H. Takayama, M. Kawatani, T. Usui, H. Osada, Application of proteomic profiling based on 2D-DIGE for classification of compounds according to the mechanism of action, Chemistry & biology, 17 (2010) 460-470.
[35] V. Menendez-Benito, L.G. Verhoef, M.G. Masucci, N.P. Dantuma, Endoplasmic reticulum stress compromises the ubiquitin-proteasome system, Hum Mol Genet, 14 (2005) 2787-2799.
[36] X. Wang, I.E. Chemmama, C. Yu, A. Huszagh, Y. Xu, R. Viner, S.A. Block, P. Cimermancic, S.D. Rychnovsky, Y. Ye, A. Sali, L. Huang, The proteasome-interacting Ecm29 protein disassembles the 26S proteasome in response to oxidative stress, J Biol Chem, 292 (2017) 16310-16320.
[37] X. Wang, C.F. Chen, P.R. Baker, P.L. Chen, P. Kaiser, L. Huang, Mass spectrometric characterization of the affinity-purified human 26S proteasome complex, Biochemistry, 46 (2007) 3553-3565.
[38] A. Borodovsky, B.M. Kessler, R. Casagrande, H.S. Overkleeft, K.D. Wilkinson, H.L. Ploegh, A novel active site-directed probe specific for deubiquitylating enzymes reveals proteasome association of USP14, EMBO J, 20 (2001) 5187-5196.
[39] P. D'Arcy, S. Brnjic, M.H. Olofsson, M. Fryknäs, K. Lindsten, M. De Cesare, P. Perego, B. Sadeghi, M. Hassan, R. Larsson, S. Linder, Inhibition of proteasome deubiquitinating activity as a new cancer therapy, Nat Med, 17 (2011) 1636-1640.
[40] S. Brnjic, M. Mazurkiewicz, M. Fryknas, C. Sun, X. Zhang, R. Larsson, P. D'Arcy, S. Linder, Induction of tumor cell apoptosis by a proteasome deubiquitinase inhibitor is associated with oxidative stress, Antioxidants & redox signaling, 21 (2014) 2271-2285.
[41] W.L. Trigona, I.K. Mullarky, Y. Cao, L.M. Sordillo, Thioredoxin reductase regulates the induction of haem oxygenase-1 expression in aortic endothelial cells, Biochem J, 394 (2006) 207-216.
[42] A.P. Intoccia, T.L. Flanagan, D.T. Walz, L. Gutzait, J.E. Swagzdis, J. Flagiello, Jr., B.Y. Hwang, R.H. Dewey, H. Noguchi, Pharmacokinetics of auranofin in animals, The Journal of rheumatology. Supplement, 8 (1982) 90-98.
[43] D.E. Furst, S.H. Dromgoole, Comparative pharmacokinetics of triethylphosphine gold (auranofin) and gold sodium thiomalate (GST), Clinical rheumatology, 3 Suppl 1 (1984) 17-24.

Figure legends

Fig. 1. Cellular response to auranofin. (A) Chemical structure of auranofin. (B) Schematic representation of reaction of auranofin. In the native state, NADPH-reduced thioredoxin reductase (TrxR) reduces thioredoxin (Trx) that in turn reduces many protein substrates within the cell. Auranofin binds the selenocysteine of reduced TrxR, leading to inhibition of the complete Trx system. (C) HCT116 cells were treated with 0.5% DMSO, 100 nM Bortezomib, 1 μM b-AP15 or 1.5 μM auranofin for 12 hours and extracts were prepared and subjected to immunoblotting using the indicated antibodies. (D) Oxygen consumption rates (OCR) were recorded in a Seahorse XF24 analyzer after the injection of different concentrations of auranofin (AUF). Data are shown as % of vehicle-treated control. Mitochondrial inhibitors were added as indicated; oligomycin is an inhibitor of ATP synthase, FCCP (carbonyl cyanide 4-(trifluoromethoxy)phenylhydrazone) is an uncoupler, rotenone is a complex I inhibitor and antimycin A is a complex III inhibitor. Note that auranofin inhibits both basal OCR and uncoupled respiration at 1 μM. Each data-point represents the mean of five samples (error bars indicate means $\pm$ S.D) (E) Extracellular acidification rates (ECAR) were recorded in a Seahorse XF24 analyzer 3 h after injection of different concentrations of auranofin. Data are shown as % of vehicle-treated control. Note that auranofin increases ECAR at 1 μM. Shown are medians and quartiles (n = 5, *** $P<0.001$; Mann-Whitney; N.S. not significant at $p < 0.05$).

Fig. 2. Auranofin induces a cellular phenotypic response distinct from proteasome inhibitors. (A) HCT116 cells were treated with 0.5% DMSO, 100 nM bortezomib, 1 μM b-AP15 or 1.0 μM auranofin for 6 hours. Lysates were prepared and processed for shotgun proteomics. Shown are fold-increases in the abundance of different proteins in drug-exposed cells relative to vehicle-treated cells. (B) HCT116 cells were treated with 0.5% DMSO, 100 nM Bortezomib, 1 μM b-AP15 or 1.0 μM auranofin for 12 hours and photographed under a phase contrast microscope. (C) MelJuSo-Ub^{G76V}-YFP/nucleus red cells were treated with different concentrations of auranofin and the signals from red nucleus were monitored and recorded in real time for 48 hours. (D) MelJuSo-Ub^{G76V}-YFP cells were treated with 1 μM b-AP15 or 1.0 μM auranofin for 48 hours. *Upper panel:* schematic illustration of Ub^{G76V}-YFP reporter system; *lower panel:* cells were tracked following drug treatment and cells that died during the 48 h observation period were identified. These dying cells were scored with regard to having become YFP positive during drug treatment. Note that whereas b-AP15 induces cell death that is strictly associated with cellular proteasome inhibition (all dying cells become YFP positive, consistent with previously results [40]), about 50% cells that died during auranofin treatment did not show YFP positivity (suggesting mechanisms of cell death unrelated to proteasome inhibition).

Fig. 3. Increases of polyubiquitinated proteins at supra-pharmacological auranofin doses. (A) HCT116 cells were treated with increasing concentrations of auranofin for 6 hours and extracts were prepared and subjected to immunoblotting using the indicated antibodies. (B) HCT116 cells were treated with 0.5% DMSO, 1.0 μM or 5.0 μM auranofin for 6 hours then followed by proteomic analysis. Total signals of chaperones (HSP90, HSPA1, HSPA4 HSPA5, HSPA6, HSPA7, HSPA8, HSPA13, HSPB1, HSPH1) were calculated and shown as fold-change (treatment vs control). Data represents were from three individual samples and was shown as minimum to maximum values (median indicated, *P<0.05, ** P<0.01).

Fig. 4. Inhibition of USP14 by supra-pharmacological doses of auranofin. (A) Auranofin does not induce dissociation of proteasomes. HEK293-Bio-Rpn11 cells were exposed to the indicated concentrations of auranofin or b-AP15 and proteasomes were purified by a biotin-tag on the 19S proteasome. Samples were processed for immunoblotting using antibodies to 19S and 20S subunits. (B) Auranofin does not inhibit 20S proteasome activity *in vitro*. Proteasomes were incubated with Suc-LLVY-AMC in the presence or absence of the indicated concentrations of auranofin. (C) HCT116 cells were exposed to auranofin or b-AP15 using the indicated concentrations. Cell extracts were labelled using the activity probe ubiquitin-vinylsulfone (Ub-VS) that binds active deubiquitinases (shown to the right). Note the inhibition of USP14 by 5 μM auranofin and 1 μM b-AP15. (D) Proteomic analysis of the response to 100 nM bortezomib, 1 μM b-AP15 and 5 μM auranofin after treatment of HCT116 cells for 6 hours.

Figure 1

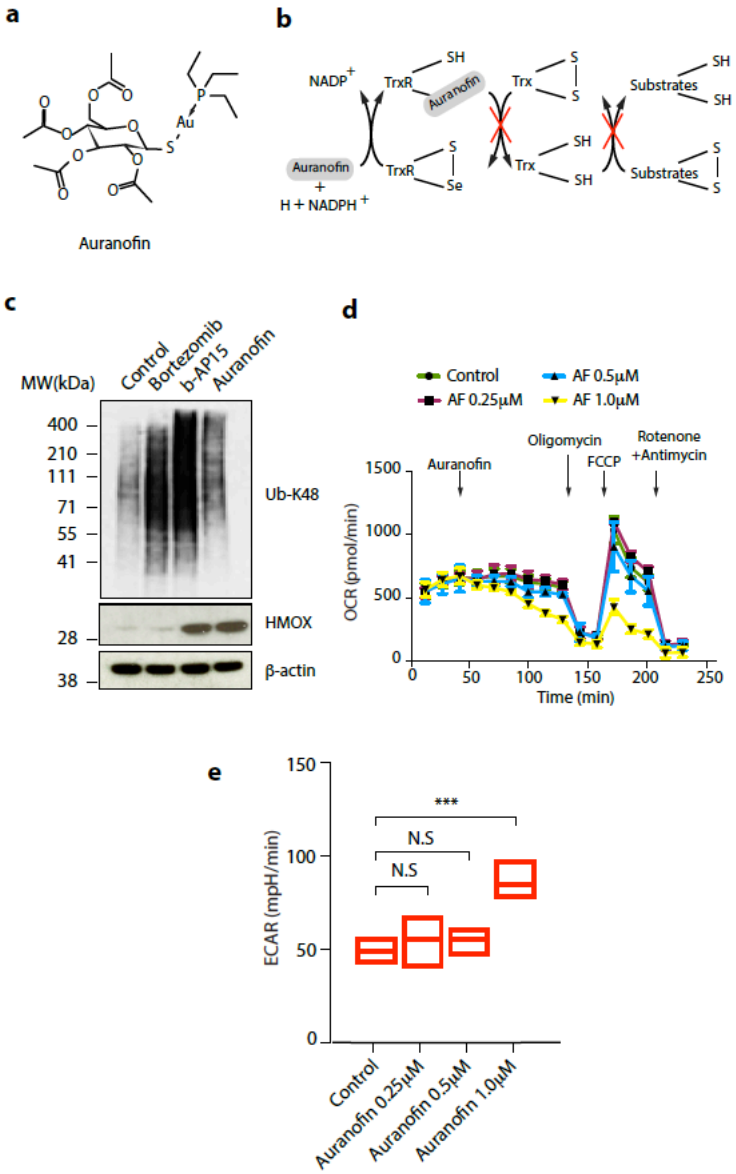
a
Auranofin
b
NADP+
TrxR
SH
Auranofin
Trx
S
S
Substrates
SH
SH
Auranofin
+
H + NADPH +
TrxR
S
Se
Trx
SH
SH
Substrates
S
S
c
MW(kDa)
Control
Bortezomib
b-AP15
Auranofin
400
210
111
71
55
41
Ub-K48
28
HMOX
38
β-actin
d
Control
AF 0.5μM
AF 0.25μM
AF 1.0μM
Auranofin
Oligomycin
FCCP
Rotenone
+Antimycin
1500
1000
500
0
OCR (pmol/min)
0
50
100
150
200
250
Time (min)
e
150
100
50
0
ECAR (mpH/min)
***
N.S
N.S
Control
Auranofin 0.25μM
Auranofin 0.5μM
Auranofin 1.0μM

Figure 2

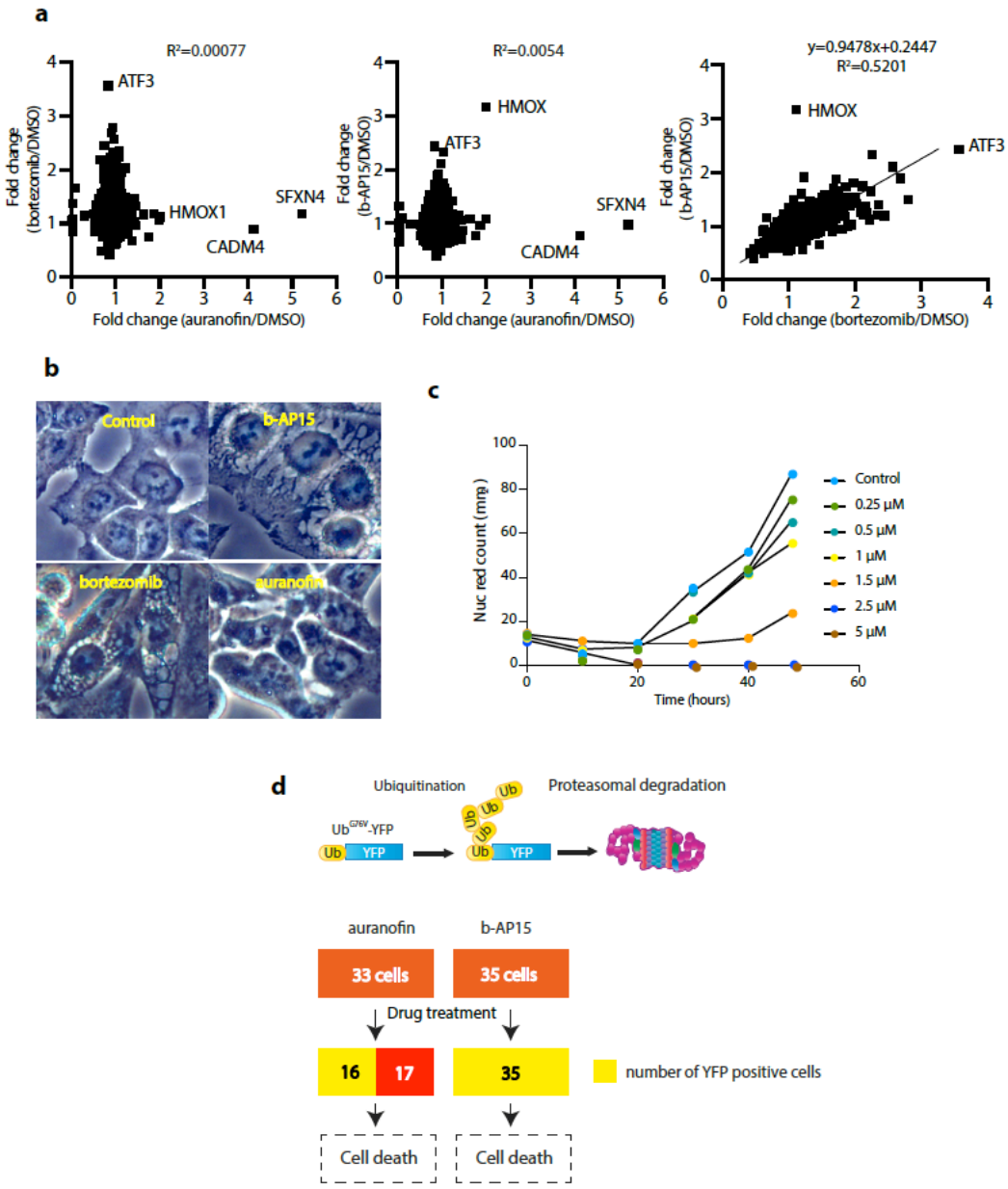
a
R²=0.00077
ATF3
HMOX1
SFXN4
CADM4
Fold change (bortezomib/DMSO)
Fold change (auranofin/DMSO)
R²=0.0054
HMOX
ATF3
SFXN4
CADM4
Fold change (b-AP15/DMSO)
Fold change (auranofin/DMSO)
y=0.9478x+0.2447
R²=0.5201
HMOX
ATF3
Fold change (b-AP15/DMSO)
Fold change (bortezomib/DMSO)
b
Control
b-AP15
bortezomib
auranofin
c
Nuc red count (mm)
Time (hours)
Control
0.25 µM
0.5 µM
1 µM
1.5 µM
2.5 µM
5 µM
d
Ubiquitination
Proteasomal degradation
Ub
YFP
auranofin
b-AP15
33 cells
35 cells
Drug treatment
16
17
35
number of YFP positive cells
Cell death
Cell death

Figure 3

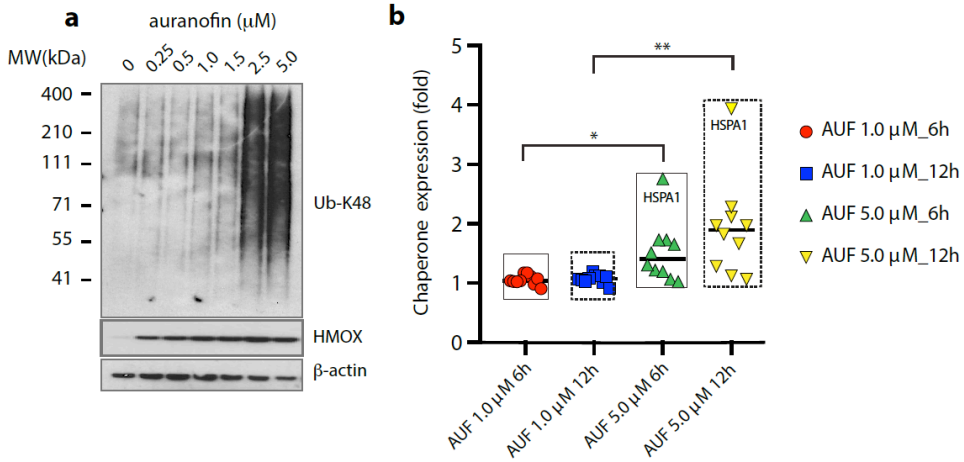
a
auranofin (μM)
MW(kDa)
0
0.25
0.5
1.0
1.5
2.5
5.0
400
210
111
71
55
41
Ub-K48
HMOX
β-actin
b
Chaperone expression (fold)
**
*
HSPA1
HSPA1
AUF 1.0 μM_6h
AUF 1.0 μM_12h
AUF 5.0 μM_6h
AUF 5.0 μM_12h
AUF 1.0 μM 6h
AUF 1.0 μM 12h
AUF 5.0 μM 6h
AUF 5.0 μM 12h

Figure 4

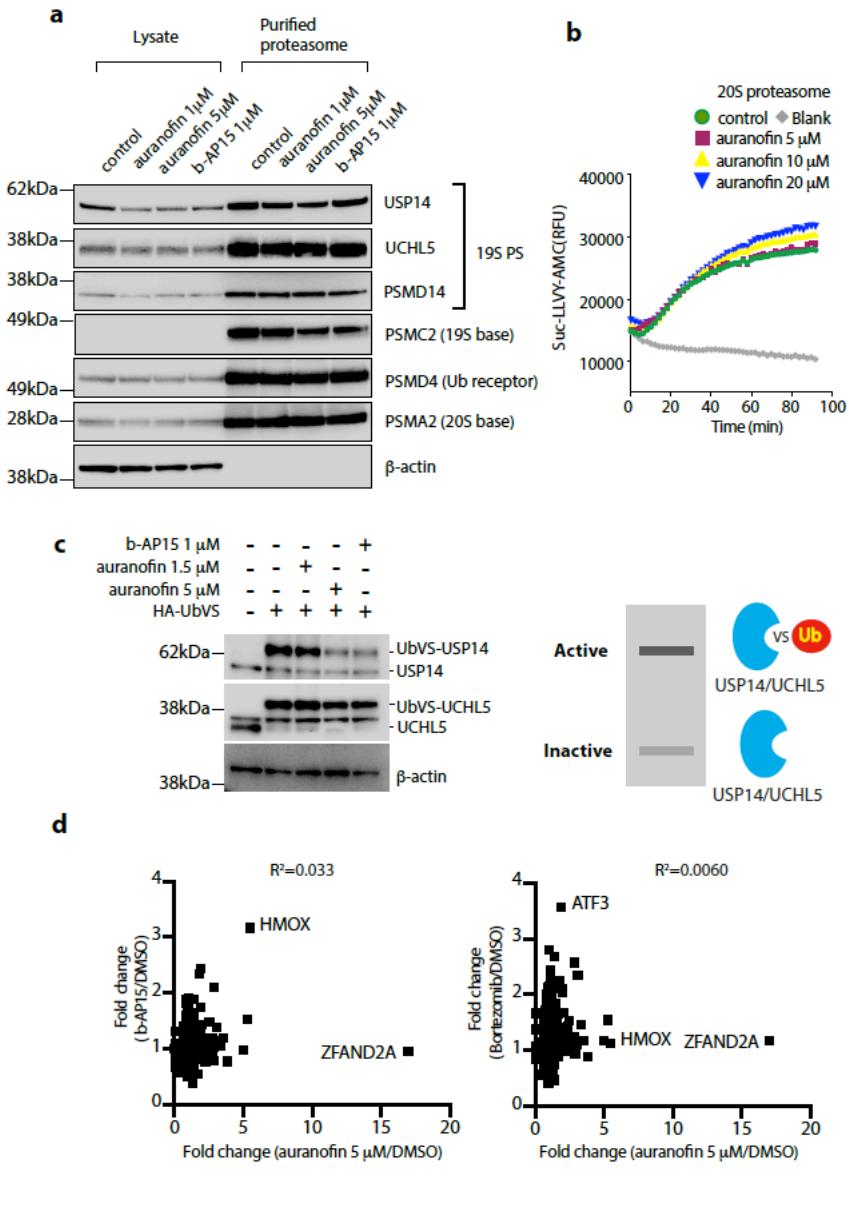
a
Lysate
Purified proteasome
control
auranofin 1μM
auranofin 5μM
b-AP15 1μM
62kDa
38kDa
38kDa
49kDa
49kDa
28kDa
38kDa
USP14
UCHL5
PSMD14
19S PS
PSMC2 (19S base)
PSMD4 (Ub receptor)
PSMA2 (20S base)
β-actin
b
20S proteasome
control
Blank
auranofin 5 μM
auranofin 10 μM
auranofin 20 μM
Suc-LLVY-AMC(RFU)
Time (min)
c
b-AP15 1 μM
auranofin 1.5 μM
auranofin 5 μM
HA-UbVS
62kDa
38kDa
38kDa
UbVS-USP14
USP14
UbVS-UCHL5
UCHL5
β-actin
Active
Inactive
VS
Ub
USP14/UCHL5
USP14/UCHL5
d
R²=0.033
HMOX
ZFAND2A
Fold change (b-AP15/DMSO)
Fold change (auranofin 5 μM/DMSO)
R²=0.0060
ATF3
HMOX
ZFAND2A
Fold change (Bortezomib/DMSO)
Fold change (auranofin 5 μM/DMSO)